The Cryosphere Discuss., doi:10.5194/tc-2016-50, 2016
Manuscript under review for journal The Cryosphere
Published: 6 April 2016

On retrieving sea ice freeboard from ICESat laser altimeter

Kirill Khvorostovsky[1], Pierre Rampal[1]

[1]Nansen Environmental and Remote Sensing Center, 5006 Bergen, Norway

Correspondence to: K. Khvorostovsky (kirill.khvorostovsky@nersc.no)

Abstract. Sea ice freeboard derived from satellite altimetry is the basis for estimation of sea ice thickness using the assumption of hydrostatic equilibrium. High accuracy of altimeter measurements and freeboard retrieval procedure are therefore required. As of today, two approaches for estimation of the freeboard using laser altimeter measurements from Ice, Cloud, and land Elevation Satellite (ICESat), referred to as tie-points (TP) and lowest-level elevation (LLE) methods, have been developed and applied in different studies. We reproduced these methods in order to assess and analyze the sources of differences found in the retrieved freeboard and corresponding thickness estimates of the Arctic sea ice as produced by the Jet Propulsion Laboratory (JPL) and Goddard Space Flight Center (GSFC). For the ICEsat observation periods (2003-2008) it is found that when applying the same along-track averaging scales in the two methods to calculate the local sea level references the LLE method gives significantly lower (by up to 15 cm) sea ice freeboard estimates over thick multi-year ice areas, but significantly larger estimates (by 3-5 cm in average and locally up to about 10 cm) over thin first-year ice areas, as compared to the TP method. However, we show that the difference over first-year ice areas can be reduced to less than 2 cm when using the improved TP method proposed in this paper. About 4 cm of the difference in the JPL and GSFC freeboard estimates can be attributed to the different along-track averaging scales used to calculate the local sea level references. We show that the effect of applying corrections for lead width relative to the ICESat footprint, and for snow depth accumulated in refrozen leads (as it is done for the last release of the JPL product), is very large and increase freeboard estimates by about 7 cm. Thus, the different along-track averaging scales and approaches to calculate sea surface references, from one side, and the freeboard adjustments as applied in the TP method used to produce the JPL dataset, from the other side, are roughly compensating each other with respect to freeboard estimation. Therefore the difference in the mean sea ice thickness found between the JPL and GSFC datasets should be attributed to different parameters used in the freeboard-to-thickness conversion.

1 Introduction

The observed thinning of the Arctic sea ice cover during the last 15 years is one of the most sensitive indicators of the climate change (e.g. Stocker et al, 2013; Laxon et al, 2013). The main data source for retrieving the sea ice thickness over large-scale basins is the radar and laser satellite altimeter measurements of the sea ice freeboard, which is used to convert freeboard to thickness assuming the hydrostatic equilibrium of floating ice (e.g. Kwok et al, 2009; Laxon et al, 2003; Laxon et al, 2013; Ricker et al, 2014; Tilling et al., 2015). Using this particular conversion method, the uncertainty of the obtained sea ice thickness is equal to ten times the one associated with the freeboard estimate. This stresses the need for very accurate altimeter measurements and freeboard retrieval procedure in order to minimize sea ice thickness uncertainty, and increase the confidence level associated to the negative trend in Arctic sea ice volume reported in the last 2013 IPCC report (Vaughan et al, 2013).

In this paper we focus on uncertainty of total (snow plus sea ice) freeboard retrieval using laser altimeter measurements from Ice, Cloud, and land Elevation Satellite (ICESat). As compared to satellite radar altimetry, ICESat provides higher accuracy in elevation measurements over a comparatively smaller footprint of ~70 m, with a precision of about 2 cm (Kwok et al., 2004). A key step in freeboard estimation process is the determination of the local sea surface height that is used as reference elevation. The determination of the local sea surface height from geoid, modelled tides, and atmospheric pressure loading is rather uncertain. Therefore, a common method is to calculate a local reference elevation from ICESat measurements over open water (or thin ice) within leads. Several methods to detect such samples were proposed in a number of studies (Kwok et al., 2007; Zwally et al, 2008; Farrell et al., 2009).

The approach proposed by Kwok et al. (2007), referred as the tie-points (hereafter TP) method, is based on identification of sea surface reference points (tie-points), for which the deviation between the measured elevation and the local mean surface exceeds a given value. Indeed, they found a relationship between surface roughness and freeboard adjacent to new lead/crack openings associated with low reflectivity, and therefore used it for tie-points detection. Later, the TP method has been further developed by Kwok and Cunningham (2008) and Kwok et al. (2009), and applied by Kurtz et al (2009) and Kurtz et al (2011) to study sea ice thickness in the Arctic. A similar approach, based on the same roughness/freeboard relationship, has been defined and used by Markus et al (2011) and Kurtz and Markus (2012) to retrieve freeboard of the Antarctic sea ice. However, one should note that the TP method has some limitations as it is based on an empirical relationship that may not be valid for some specific time and location.

Another approach, the so-called lowest-level elevation (hereafter LLE) method, was originally described and used in a study by Zwally et al. (2008) and later applied by, for example, Yi et al. (2011) or Kern and Spreen (2015) to retrieve freeboard of Antarctic sea ice, and by Yi and Zwally (2009) for the Arctic sea ice. The LLE method is based on selecting a certain percentage of the lowest elevation measurements within the along-track section surrounding every ICESat sample, and assumes that their mean represents the local sea surface height for the given sample. A main limitation of the LLE method is that in case of absence of leads or cracks in the vicinity of a given measurements or if the selected percentage of lowest elevations is larger than the actual number of measurements over leads/cracks, the level of sea surface is overestimated, and consequently the freeboard is underestimated.

Comparison of available thickness products derived by Jet Propulsion Laboratory (JPL) using the TP method (http://rkwok.jpl.nasa.gov/icesat) and by Goddard Space Flight Center (GSFC) using the LLE method (Yi and Zwally, 2009) shows that part of the difference between the estimates can be attributed to the uncertainty of the freeboard-to-thickness conversion and in particular to the chosen value for ice density (Zygmuntovska et al, 2014). Lindsay and Schweiger, (2015)

The Cryosphere Discuss., doi:10.5194/tc-2016-50, 2016
Manuscript under review for journal The Cryosphere
Published: 6 April 2016

found that JPL estimates are thicker on average than those in the GSFC product by 0.42 m, and proposed that it can be caused by the different techniques for determining the local sea level in the freeboard retrieval algorithm, and by the different methods in estimating snow depth that is used when calculating ice thickness.

In this paper we reproduce the two approaches used to retrieve Arctic sea ice freeboard, i.e. using the TP and LLE methods. We analyze why these methods lead to differences in local freeboard estimates, show how they are distributed in space and over the ICESat period (2003-2008), and propose an improvement in the freeboard retrieval algorithm used in the TP method. The TP method presented originally in Kwok et al. (2007) was further developed and improved to take into account snow that is accumulated on thin ice in leads (Kwok and Cunningham, 2008) and size of leads with respect to the size of the ICESat altimeter footprint (Kwok et al., 2009). The effect of these two corrections on freeboard estimates, and hence on the difference between the corresponding sea ice thickness products, is also quantified.

2 Data and methods

2.1 Data

In this study we use the ICESat level 2 data of Release 32 from 10 laser campaigns, corresponding to periods of ~35 days in autumn and winter named as 2a , 2b , 3a , 3b , 3d , 3e, 3g, 3h, 3i and 3j in the ICESat dataset and that we will hereafter denoted with respect to the period covered as ON03 (i.e. October-November 2003), FM04, ON04, FM05, ON05, FM06, ON06, MA07, ON07, FM08. We also use along-track freeboard estimates derived from ICESat (Yi and Zwally, 2009) and available for download on the NSIDC server (http://nsidc.org/data/nsidc-0393).

In addition, we use the Arctic-wide multiyear ice fraction dataset used in Zygmuntowska et al. (2014) that was produced by reprocessing the QuikSCAT satellite scatterometer data using the method described in Kwok (2004), in order to get daily estimates. We also use the NSIDC, daily, 25-km-resolution sea ice concentration product based on Advanced Microwave Scanning Radiometer (AMSR-E) satellite measurements.

2.2 ICESat data filtering and corrections

Unreliable ICESat elevation estimates were filtered out using waveform parameters of the altimeter returns provided together with ICESat data. We used the criteria applied in Kwok et al. (2007) when reproducing both methods in order to compare the algorithms avoiding biases associated with different filtering. We discarded measurements where the receiver gain used for indicating forward scattering in the atmosphere (i_gval_rcv) was more than 30 and the standard deviation of the difference between received ICESat echo waveforms and the Gaussian fit (i_SeaIceVar) was more than 60. Saturated waveforms occurred over bright smooth flat surfaces with reflectivity (i_reflctUC: ratio between received and transmitted energy) >1 were removed. In addition, we filtered out highly saturated returns with amplitude greater than the saturation index threshold for more than five consecutive waveform gates (i_satNdx > 5). The influence of the filtering criteria on freeboard estimates will be illustrated below in an example where we apply a different threshold for the receiver gain parameter (80, as used by Yi and Zwally, 2009).

Then we determine the elevation, h, above the EGM08 geoid (Pavlis et al., 2012) provided with the ICESat data, and apply saturation correction to the measurements with moderately saturated waveforms using the corresponding parameter (i_satElevCorr) and flag (i_satCorrFlg), as well as the inverse barometer correction to allow for atmospheric pressure loading (Kwok et al., 2006, Zwally et al, 2008). We discard the areas with open ocean, which we define here as the region covered by less than 30% sea ice coverage, according to the AMSR-E ice concentration product from NSIDC.

It should be noted that Kwok et al. (2007) and Yi and Zwally (2009) used ICESat data from the earlier Release 28 and estimated elevations, h, above the ArcGP geoid (http://earth-info.nga.mil/GandG/wgs84/agp/hist_agp. html) rather than the EGM08 geoid. Furthermore, when applying the LLE method Yi and Zwally (2009) first calculated the improved geoid before using it for freeboard estimation. Although freeboard retrieval from satellite altimetry is primarily based on estimation of local sea level in leads the effect of using a different geoid on the results is evaluated in the section 3.2.

2.3 Algorithms used in the TP and LLE methods

In order to remove longer wavelength and large amplitude variability due to geoid, atmospheric loading and tidal errors, the first step for both (TP and LLE) freeboard retrieval algorithms is to determine relative elevations, h_r, defined as the difference between elevations h and their 25-km (like in Kwok et al., (2007)) or 50-km (like in Yi and Zwally, (2009)) running means, $\bar{h}$, as $h_r = h - \bar{h}$. The effect of the different scale of spatial smoothing when calculating $\bar{h}$ is evaluated and discussed in section 3.2.

The principal distinction between the algorithms, as noted above, is the difference in the method used to determine the sea surface references. For the LLE method, Yi and Zwally (2009) assumed that the lowest 1% of the measurements along the satellite track represent elevations over open leads and therefore can be used for estimation of the local sea level. Hence, they determine elevations of sea level, h_{sl}, as the mean of the 1% lowest h_r values within ± 50 km around each measurement point. Therefore, in this approach the number of points used for the determination of sea level depends only on measurements' availability. Since the distance between ICESat samples along track is 172 m, and if we assume that all samples are reliable, 6 of about 600 measurements within the 100-km range are used to calculate the local sea surface level. However, in case there is no open water within the 100-km range, the calculated h_{sl} will be the height of thin ice rather than the sea level height, leading to an underestimation of the sea ice freeboard.

For the TP method, Kwok et al. (2007) determined sea level from ICESat samples, tie-points, identified accordingly to specified requirements. From the analysis of satellite images, Kwok et al. (2007) found a linear relationship between along-track elevation variability and freeboard values adjacent to new openings at the same locations where leads were identified and collocated with ICESat data. Although determination of this relationship provides a tool for detection of tie-points, the procedure of visual inspection of satellite images is time-consuming, and can be applied only for regional analysis (e.g. Markus et al., 2011). Therefore Kwok et al. (2007) proposed to use the relationship between elevation variability and negative h_r with dips in reflectivity, which are found to be associated with young ice in leads. Elevation variability is defined as the standard deviation σ_{25} of the detrended h_r within a 25-km running window. The dips in reflectivity are defined as when the difference between the local reflectivity for a given sample and the background reflectivity, ΔR, is larger than 0.3. The background reflectivity is estimated as the average reflectivity of all the measurements within 25 km around a given sample that are greater than $\bar{R} - 1.5\sigma$. Then they select all samples corresponding to the points below the line obtained from a regression model, here a cubic polynomial, to be used as tie-points. That is, they select samples for which σ_{25} is less than that determined from the cubic polynomial model for the given h_r. Kwok et al., (2007) identified two sets of tie-points: one set consists of samples located below the regression model which also have $\Delta R > 0.3$, and the other one includes all the samples corresponding to the points located below the regression model without constraining the value of ΔR. They found good agreement between these two sets of tie-points as well as their agreement with high-quality tie-points determined from collocation with satellite images. Since the number of tie-points in the former set is not sufficient for the basin-wide studies, both sets of detected tie-points are used for the calculation of sea level. The sea surface references are estimated for 25-km non-overlapping segments as an average of h_r values corresponding to the tie-points, weighted as the exponential function of the distance to the line obtained from the regression model. The higher σ_{25}, which is characteristic of the roughness around given sample, the lower h_r is required to be for this sample to qualify as a tie-point. This weighting method of the tie-points utilizes their likelihood to be a reference point, and is particularly important when many tie-points are detected within a 25-km segment. Since the position of the line issued with the regression model varies over seasons and years, Kwok et al., (2007) proposed to apply the same regression model separately for each ICESat observation period. Influence of the chosen regression model is discussed in the section 3.3.

2.4 Correction of geoid

In Zwally et al. (2008) and Kwok et al. (2007) a difference between running mean elevations, $\bar{h}$, and the determined elevation of sea level, h_{sl}, was found in order to characterize the unresolved residuals in the sea surface height. Since the spatial pattern of the differences is found to be consistent for different ICESat campaigns these residuals were mainly associated with the characteristics of uncertainties in the static geoid, and to a less degree as coming from time-varying components or noise in the freeboard estimation process. Therefore Yi and Zwally (2009) applied this difference, $\bar{h} - h_{sl}$, to correct geoid heights, and used this new improved geoid for retrieving the freeboard. We determined the differences $\bar{h} - h_{sl}$ for each along track measurement, and examined the effect of this geoid adjustment on freeboard estimates in section 3.2.

2.5 Adjustments for snow depth and area of sea surface references

After being presented in Kwok et al. (2007) the TP method for freeboard retrieval was further developed by implementing two corrections of sea surface references based on functions determined empirically. One correction is an adjustment of the elevations in tie-points for taking into account the depth of snow accumulated over young ice (Kwok and Cunningham, 2008). This adjustment is based on the contrast difference in reflectivity existing between sea ice and snow surfaces, and is estimated as a function of $(1-\Delta\mathrm{R})$. The correction of the sea surface references varies within the range 0 to 5 cm (Fig 2b in Kwok and Cunningham (2008)).

Another correction accounts for the fact that ICESat measurements over tie-points are contaminated by the neighboring sea ice surface within the laser altimeter footprint. In Kwok et al. (2009), it was proposed to multiply all the freeboard measurements by a factor of $1.1+0.1\left(\frac{R_{snow}-R}{R_{ow}}\right)$, where $R_{snow}=0.7$ and $R_{ow}=0.25$ are the typical reflectivity of snow and ice respectively, and R is the reflectivity of the ICESat measurements. This correction increases with freeboard height and decreases with the reflectivity in ICESat samples.

3 Results and discussion

In this section we compare different freeboard estimates retrieved using our implementations of the TP and LLE methods. First, we test the agreement between freeboards obtained using our implementation of the LLE method and those provided in the GSFC product. Then, we analyze how the choice of different along-track averaging scales and geoid definition affect the freeboard estimates when using the TP and LLE methods, and therefore how it can partly explain the differences found between the JPL and GSFC products. We also quantify the effect of applying different approaches for determination of sea surface references in the TP and LLE methods when choosing the settings, which give consistent freeboard retrievals. Based on these analyses we propose an improvement of the freeboard retrieval algorithm used in the TP method. We also estimate the effect on freeboard estimates of applying corrections accounting for snow depth in tie-point areas and for the size of leads, as it was done for the last release of the JPL product. Finally, we proceed with a comparison of the obtained freeboard when using the different methods and parameters, and we summarize our findings.

3.1 Comparison of GSFC product with freeboard retrieved using the LLE method

We checked consistency between the freeboards retrieved in this study and those available from the GSFC product by following the LLE method described in Yi and Zwally (2009): the elevations were used relative to the ArcGP geoid corrected for $\bar{h}-h_{sl}$ residuals, the calculation of $\bar{h}$ values was made using an along-track smoothing window of 50-km, and the 1% lowest elevation measurements over the 100-km along-track segment centered on each sample were used for estimation of the reference sea level h_{sl}. We compared our results with the freeboards of the GSFC product by first computing the differences between the freeboards calculated along track for each sample before computing their averages over a regular 25-km grid covering the data domain. Maps of freeboard estimates as well as maps of differences and their distribution for the ON05 and FM06 ICESat periods are presented in Figure 1. The mean and standard deviation of the differences for the other periods are recapped in Table 1 (first line). The mean differences are small, i.e. around ±2 cm, indicating good agreement between the estimates. The remaining discrepancies can be attributed to different data filtering, and partly to the differences existing between data releases.

In particular, persistent underestimation of the freeboard thinner than 15 cm by up to 10 cm for the ON05 and FM06 periods (Figure 1b and 1d) can be explained by different threshold values used for the receiver gain parameter. Indeed, following Kwok et al. (2007) we used ICESat measurements with the gain values of less than 30, while Yi and Zwally (2009) chose to set this threshold value to 80, thereby involving more data in their analysis. This additional portion of the data is more affected by atmospheric forward scattering, leading to measurements showing a larger range and shifted towards lower elevation values. For thin ice the likelihood is high for these elevations to be lower than the neighboring ones along the track, and as a consequence for them to be used for determination of sea surface reference, which may finally result in higher freeboard estimates. We checked that applying the exact same threshold as in Yi and Zwally (2009) for the receiver gain parameter increases the agreement between the estimates, as one can see from the removal of the very negative (in blue) differences present over the Kara, Laptev and Chukchi Seas in the maps of Figure 1c as compared to the maps of Figure 1b. One should note however that in addition Yi and Zwally (2009) used a pulse-broadening parameter for the data filtering that is not applied here. This parameter primarily depends on the width of the echo waveform and, among other effects, accounts also in part for atmospheric forward scattering. This explains why we obtain a noticeably higher freeboard as compared to the GSFC product for some ICESat periods like e.g. ON03 and ON04 when setting the threshold value for receiver gain to 80 (Table 1, second line). Thus we think that setting the threshold value for receiver gain to 30 is roughly equivalent to the filtering settings applied by Yi and Zwally (2009) to account for forward scattering, but has the advantage of being more efficient over regions of thin ice.

3.2 Sensitivity of freeboard estimates to LLE method parameters and geoid definition

The JPL and GSFC products, as noted above, are generated using different along-track averaging scales to calculate $\bar{h}$ values, i.e. 25 and 50-km respectively. The length of the along-track segment used for estimation of the local sea level references h_{sl} is also different: 1% of lowest elevations available over 100-km around each sample for the GSFC product (YI and Zwally, 2009), while 25-km non-overlapping segments are used for the JPL product (Kwok et al., 2007). Therefore, before comparing the freeboard retrievals obtained with the two methods we checked, as an example, how the choice of different averaging scales influence the results when using the LLE method. Although both freeboard retrieval algorithms are based on the difference between ICESat elevations over sea ice and the neighboring leads, which makes them almost fully independent from the geoid accuracy, we also looked at how the choice of geoid influences the results.

We compared the freeboards retrieved using the LLE method with a window's size of 25-km and 50-km to compute $\bar{h}$, and using along-track averaging segments of 25-km and 100-km to estimate h_{sl}. Note that these averaging scales correspond to those used to produce the JPL and GSFC freeboard estimates. Using the JPL versus GSFC scales into the LLE method results in freeboard differences of about 4 cm (Table 1, line 3 and Figure 2a for the FM06 period). By applying other combination of averaging scales we found that these differences are actually mainly coming from the use of different h_{sl} values. This is expected from the fact that considering a larger window increases the chance to include lower h_r dips in the calculation of h_{sl}. Freeboard differences due to different averaging scales for calculation of $\bar{h}$ are small and their patterns are similar to those related to geoid uncertainty shown in Figures 2b and 2c. A positive bias in freeboard estimates when using longer segments for along-track averaging is also reported in Kern and Spreen (2015) for the Weddell Sea in Antarctica. One should also note that freeboard differences associated with along-track averaging scales are dependent on the surface roughness, which is confirmed by looking at the period FM05 when the largest values of σ_{25} are observed (Table 1, line 3 and Figure 5a).

The residuals $\bar{h} - h_{sl}$ applied for the correction of the ArcGP geoid are calculated using the same settings as in Yi and Zwally (2009) and shown in Figure 2d for the period FM06. The spatial distribution of the residual is similar for the other periods and is in agreement with those obtained by Kwok et al (2007). The effect on freeboard estimates is small, ranging within ±2 cm, over most of the Arctic basin (Figure 2b). The only noticeable effect on freeboard is found in the areas of the Gakkel and Lomonosov ridges, where freeboard is reduced by about 5 cm. The areas of positive differences along the East Greenland and Canadian Arctic coasts correspond to regions of largest freeboard (Figure 1a), which is itself correlated with local surface roughness (Figure 5a), more than to the distribution of the geoid correction. The $\bar{h} - h_{sl}$ adjustment of EGM08 geoid is proportionally lower everywhere in the Arctic by about 13 cm, which corresponds to the higher level of the EGM08 geoid (Figure 2d). The effect of adjustment of the EGM08 geoid for $\bar{h} - h_{sl}$ on the freeboard is of the same order in means (Table 1, line 4) and even less evident along the ridges in the central Arctic, which likely results from the overall better quality of this more recent geoid, and in particular from the better representation of small scale features. Small freeboard differences are also obtained when using the EGM08 instead of the ArcGP geoid (Table 1, line 5). In addition to the local effect along the ridges in the central Arctic the improvements in the EGM08 geoid are revealed in other areas such as along the high slopes of the bathymetric relief (see Figure 2c for the FM06 period).

Thus in order to assess the effect of different algorithms applied for determination of h_{sl} in the LLE and the TP methods the same scales for along-track averaging should be used to avoid corresponding bias. In order to avoid this bias when comparing the LLE and TP methods, we chose to use an averaging window of 25-km to calculate $\bar{h}$ and h_{sl} (as in Kwok et al., 2007) for the two following reasons. Using a smaller window is found to result in reduced dependency of the freeboard on the geoid used in the retrieval process. Indeed, in this case the correction of the geoid for $\bar{\mathrm{h}} - \mathrm{h}_{\mathrm{sl}}$ as well as the fact of using a recent geoid like EGM08 no longer has any impact on freeboard along the ridges in the Arctic, as opposed to what we reported above when using larger spatial averaging. Another reason is that, as demonstrated by Kern and Spreen (2015), a more valid freeboard can be retrieved using the LLE method if the length of along-track segments considered for the selection of the lowest elevations when estimating the local sea level reference h_{sl} is equal to, or less than, the size of the smoothing window used to calculate $\bar{h}$ values. As the number of ICESat measurements available within each 25-km section does not exceed 147 samples, and most often even less due to data filtering, for each section the 1% of the measurements considered as the lowest h_{r} values and used for estimation of h_{sl} actually refer to only one sample. Kern and Spreen (2015) suggested that using such a low percentage and consequently such a low number of samples to estimate the local sea level reference may result in freeboard overestimation if sharp elevation changes are present along the track. However, this only happens if the size of the averaging window used to calculate $\bar{h}$ is smaller than the length of the segment used to estimate the local sea level reference h_{sl}, which is not the case here since we use the same 25-km averaging scales for estimation of $\bar{h}$ and h_{sl}.

3.3 Comparison of sea ice freeboard obtained by using TP and LLE methods

3.3.1 The original algorithm used in the TP method

A comparison of sea ice freeboards calculated using the LLE and TP methods when applying the same along-track averaging scale as described in the previous section is presented in Figure 3. Differences between freeboards are estimated separately for the first-year ice (FYI) and multi-year ice (MYI) regions over the same 25-km grid cells. Grid cells are considered as covered with FYI or MYI according to the 50% isopleth on the multi-year ice fraction maps that were derived by Zygmuntowska et al. (2014) from QuikSCAT scatterometer following the method described in Kwok (2004). The obtained freeboard differences are small on average, ranging within ±5 cm, while the presence of significant regional discrepancies should be noted.

Negative differences, which corresponds to lower freeboard being retrieved using the LLE method as compared to the TP method according to the convention used here, are found for areas covered by MYI and located north of Greenland and Canadian Arctic Archipelago. The largest negative differences are observed for the period FM08 and are about -15 cm. These can be explained by the fact that in these areas of thick ice the TP method does not detect any leads for many 25-km segments, while the LLE method provides freeboard estimates because it calculates a local sea surface reference from the 1% lowest elevations that are not necessarily representative of local sea level. One can also expect basin-wide difference between the freeboard estimates in the area of thick MYI to be even larger when the TP method does not detect any tie-points within some 25-km grid cells and, hence, does not provide freeboard estimates. We therefore conclude that the difference found between the results of these two methods in areas of MYI is coming from (i) the lower-biased estimates due to a poor constrain on the calculation of local sea level references in the LLE method or (ii) the absence of local detection of tie-points in the TP method, mainly where the ice cover is continuous, i.e. with only few or no leads.

Positive differences are obtained over large areas of FYI for most of the ICESat campaigns, with a peak in FM08. The mean differences over FYI are within 3-5 cm, while locally these can be more than 10 cm. Since the lead fraction in the areas of seasonal ice is higher than over thick MYI, one can expect that the observed difference in freeboard estimates is not coming from the same reasons mentioned above for MYI areas. In order to explain the source of differences over FYI areas we investigated the performance of the algorithm used in the TP method. The results are presented in the next section.

3.3.2 An improved algorithm for the TP method

In the TP method, as described in section 2.3, one has to find the samples that will be used as tie-points. To do so, we first establish the relationship between $\mathrm{h_r}$ and σ_{25} using a regression model for the measurements showing dips in reflectivity (a cubic polynomial function in Kwok et al., 2007). Figure 4 shows the relationship found between $\mathrm{h_r}$ and σ_{25} for the ten ICESat campaigns. We checked that our results were in agreement with those of Kwok et al. (2007). Then, according to Kwok et al. (2007), the tie-points can be defined by taking the samples found to be below the regression curves. The number of detected tie-points within each 25-km non-overlapping segments ranges from a few tie-points (i.e. < 10) over thick MYI to several tens (i.e. > 25) over FYI (Figure 5b) and has a significant spatial variation. The sea level reference for each 25-km segment is estimated by averaging the $\mathrm{h_r}$ values corresponding to the tie-points, weighted exponentially by the distance from the regression model (Kwok et al., 2007). Hence, the contribution of tie-points with larger distances dominates when calculating the local sea level reference. The σ_{25} values are smoothed along-track and do not change remarkably over the segment, while $\mathrm{h_r}$ may vary significantly from sample to sample. The tie-points with lower $\mathrm{h_r}$ contribute more than those with larger $\mathrm{h_r}$ for a given σ_{25}. However, one can note that when going toward $\mathrm{h_r} = 0$ the linear correlation existing between $\mathrm{h_r}$ and σ_{25} is lost as it can be seen from the flattening of the curves in Figure 6a. In FM08 this correlation becomes even inversed with an inflection point around $\mathrm{h_r} = -5$ cm. When using a cubic polynomial fit of the data as in Kwok et al. (2007), the correlation does not hold towards small $\mathrm{h_r}$ for all periods, and shows an inversed correlation for FM08, or at least a flattening, as for FM05 (see red dashed lines in Figure 6a). As a consequence, the samples detected as tie-points that have a value of $\mathrm{h_r}$ close to zero (i.e. measurements taken over areas covered by thin ice) may contribute more than the other, leading to an artificial increase of the reference sea level height over given segments. Note that the fact that the relationship between σ_{25} and $\mathrm{h_r}$ does not hold for thin freeboard can be explained by a lower likelihood for samples with $\Delta\mathrm{R} > 0.3$ to represent actual leads. This is illustrated by the increase of the standard deviation of σ_{25} and the decrease in number of samples used in evaluating σ_{25} for low absolute values of $\mathrm{h_r}$ (Figure 6b and 6c, red).

Underestimation of the freeboards retrieved over thin FYI by the TP method as compared to those retrieved from the LLE method increases with the number of samples detected as tie-points and with surface roughness. This can be explained from the fact that a large number of tie-points or a high degree of roughness increase the chance that some of those tie-points would be associated with the flattening part of the curve relating σ_{25} and $\mathrm{h_r}$. In general, the number of tie-points and roughness are anti-correlated and their spatial patterns match very well with the pattern of multi-year versus first-year ice as shown in Figure 5 for the FM05, ON05, FM06 and FM08 ICESat periods. For example, differences of freeboard estimates are related to surface roughness in FM05 and number of detected tie points in FM08.

In order to reduce such bias and to ensure that the selected samples used to establish the relationship between σ_{25} and $\mathrm{h_r}$ are actually over leads we propose an improvement to the TP method. This improvement is based on further constraining the method of selection of samples by requesting that dips in both reflectivity and elevation need to be actually measured. Here, we select samples with $\Delta\mathrm{R} > 0.3$ and $\mathrm{h_r} < \overline{\mathrm{h_{r25}}} - 0.5\sigma_{25}$, i.e. samples where $\mathrm{h_r}$ deviates from the 25-km running mean $\overline{\mathrm{h_{r25}}}$

by at least half of a standard deviation. For $h_r < -15$ cm the resulting relationships between σ_{25} and h_r is very similar to the one obtained for the previous selection of samples, while for $h_r > -15$ cm both the high variability and inverse distribution are removed (Figure 6a, black). Since applying additional requirements on the selection of samples considered in the data regression reduces their number, especially for near zero h_r, we only consider as reliable the (1-cm) h_r bins for which σ_{25} is estimated from at least 15 samples. It should be noted that despite the actual lower number of samples selected with this new method the variability of σ_{25} is significantly decreased, and the relationship between h_r and σ_{25} over thin ice remains robust over the whole range of h_r and σ_{25} values. Note that we also tried to apply more stringent selection requirement on the elevation dips like e.g. $h_r < \overline{h_{r25}} - \sigma_{25}$ and $h_r < \overline{h_{r25}} - 1.5\sigma_{25}$. In this case, the resulting $\sigma_{25} = f(h_r)$ relationships (Figure 6a cyan and blue lines, respectively) are shifted downward compared to the previous one obtained when requiring $h_r < \overline{h_{r25}} - 0.5\sigma_{25}$ (Figure 6a, black line). These lines represent rather the relationships of the mean σ_{25} that Kwok et al. (2007) obtained using collocation of the satellite images with ICESat data, which we mentioned above in the section 2.3. From this analysis, using the condition $h_r < \overline{h_{r25}} - 0.5\sigma_{25}$ in this improved TP method appears to be the most appropriate.

We tested our new TP method on the whole ICEsat dataset using the additional constrain $h_r < \overline{h_{r25}} - 0.5\sigma_{25}$ in the procedure of selection of samples used to form relationships between h_r and σ_{25}. The difference between the freeboards retrieved with the new-TP and LLE methods (Figure 7) is now largely reduced over FYI. Depending on the period considered, the mean difference is now varying from 1.5 cm to 3.1 cm (1.6 cm to 3.3 cm for FYI) as compared to 2.4 cm to 4.4 cm (2.5 cm to 5.3 cm for FYI) before, while the range of standard deviation of the differences remains similar. As expected, the differences remain unchanged for MYI since our modification of the TP method only impact freeboard estimate over thin ice areas.

3.4 Impact of snow depth in leads and lead size adjustments on sea surface reference calculation

Corrections to account for snow depth at the location of tie-points (which are supposedly leads) and for the size of leads with respect to the size of ICESat footprint (as proposed and applied by Kwok and Cunningham (2008) and Kwok et al. (2009)) is another source of contribution to the differences between the sea ice thickness products from the JPL and GSFC. The adjustment of freeboard included in the TP algorithm and related to snow depth in refrozen leads is about +2-3 cm and rather uniformly distributed over the Arctic (Table 2, first line and Figure 8a for ICESat periods ON05 and FM06). The other adjustment of freeboard related to the fact that lead area does not cover the entire ICESat footprint at the locations where tie-points are detected is applied after the adjustment for snow depth previously mentioned. The magnitude of that second correction is primarily correlated to freeboard height and ranges from +3 to +7 cm on average over the Arctic depending on the period considered. Indeed, we observe that this correction is less important for the ICESat periods from and after ON05, i.e. when sea ice thickness starts to reduce significantly (Table 2, second line). Example of spatial distribution of that correction for the periods ON05 and FM06 is shown in Figure 8b. We can see that the largest corrections are observed over

MYI areas. Depending on the ICESat period considered, the mean of that correction vary from 3.7 to 9.3 cm and from 2.3 to 5.6 cm over MYI and FYI areas, respectively.

The sum of these two corrections is about +7 cm on average over the Arctic and over the ICESat period, and ranging from 5 to 10 cm depending on the particular period. Note that the mean corrections reported in Table 2 are estimated using the original TP method, and that we found very similar results when using the improved TP method that we propose in section 3.3.

3.5 Summary

Mean sea ice freeboard calculated over the whole arctic basin using different methods is shown in the Figure 9. The figure includes freeboard estimates from the GSFC product, estimates we calculated using the same LLE method (but with finer resolution along-track averaging), those we calculated using the original TP method as described in Kwok et al. (2007), and those calculated using the improved TP method we propose in this study, with or without adjustments for snow depth and leads width. Note that for consistency in the comparison we computed mean values of freeboard by only considering grid cells where estimates were available for all these methods.

Because of the use of different averaging scales to calculate sea level references, the sea ice freeboards we estimated using the LLE method are lower by ~4 cm on average as compared to those of the GSFC product for all ICESat periods. Sea ice freeboards we estimated using the original TP method are lower by ~3 cm on average as compared to those we obtained using the LLE method with identical along-track averaging scales. Although the TP method has the advantage of avoiding bias due to the use of samples over sea ice to calculate the local sea level reference, and prevent from local underestimation of the freeboard in thick ice areas, it may underestimate freeboard estimates over the large areas covered by thin ice. Also, the freeboards obtained by the TP method are lower over MYI for the first three ICESat periods (ON03, FM04 and ON04) where medium-thick freeboard of about 30 cm is observed.

The lower average freeboard retrieved by the TP method can be explained by using the large number of tie-points found in thin ice areas. Although the tie-points with lower elevations have greater weight in most cases the resulting sea surface reference is biased positive, hence leading to lower freeboard estimates. This was already seen in Kwok et al. (2007) as the freeboard retrieved by the TP-method for ON05 and FM06 periods were, in average, lower by 1.3 to 4 cm as compared to freeboards neighboring to leads detected in parallel on satellite images and collocated with ICESat data. However, the difference between freeboards retrieved by the LLE and TP methods is reduced by more than 30% for the whole Arctic and by 40% for FYI when applying our suggested improvements of the algorithm used in the TP method.

The adjustments for snow depth in leads and leads width were applied only when producing the JPL dataset, and we estimated that their combined effect increases freeboard by about 7 cm. Since the ratio between mean sea ice freeboard and thickness reported in Kwok et al. (2009) is about 6, the application of these two adjustments could be in principle sufficient to explain the difference of 0.42 m on average found between the JPL and GSFC sea ice thickness products (Lindsay and

Schweiger, 2015). However our results show that after applying both corrections the freeboards retrieved using the original and improved TP method are, on average, similar and higher by ~1 cm respectively, as compared to the GSFC product.

As sea ice freeboard data from JPL are not available we cannot check their consistency with those estimated for this study using the same method, or provide a comparison with the estimates provided in the GSFC product. According to our findings the freeboards of the GSFC product and those that were most likely calculated at JPL are close in average, meaning that the difference between the JPL and GSFC averaged sea ice thicknesses are probably coming from the difference in the choice of parameter values used in the freeboard-to-thickness conversion.

Conclusions

In this paper we reproduced two methods already used in other studies to retrieve sea ice freeboard using ICESat data, called the lowest level elevation (LLE) and tie-points (TP) methods. The main difference between retrieval algorithms used in these two methods reside in applying different approaches to determine the local sea level references – a key step in the process of estimating sea ice freeboard. Two available products of the Arctic sea ice thickness, GSFC and JPL, were derived respectively from freeboards retrieved with these two approaches, but were found to differ significantly, i.e. by 0.42 m (Lindsay and Schweiger, 2015). In this study we analyzed the possible reasons for freeboard discrepancies when using the LLE and TP methods as well as their contribution to the observed thickness difference.

We first reproduced the freeboard estimates of the GSFC product by using the algorithm of the LLE method. We estimated the contribution of using different along-track averaging scales in the TP and LLE methods (as it is the case between Kwok et al. (2007) and Yi and Zwally (2009), respectively) on the freeboard estimation and how it could possibly explain the sea ice thickness differences found between the JPL and GSFC products. The along-track averaging scales used by Yi and Zwally (2009) are larger than those used by Kwok et al. (2007), resulting in higher freeboard estimates by ~4 cm in average. We also estimated the effect of the geoid adjustment applied by Yi and Zwally (2009) for the residuals between the geoid heights and the sea level determined from ICESat data. In this analysis, noticeable freeboard differences are observed only locally, i.e. along the high slopes of the bathymetric relief, and only when using large along-track averaging scale.

In order to analyse the effect of using different approaches to estimate local sea level references, the same 25-km along-track averaging was applied for both the LLE and TP methods. Our results show that locally and over thick MYI areas with very few leads the LLE method gives a lower sea ice freeboard by up to 15 cm when compared to the TP method. Over FYI, in contrast, the LLE method gives sea ice freeboards that are higher by 3-5 cm in average compared to the TP method. This can be explained by the large number of ICESat samples selected for calculating local sea level and their inadequate weighting in these calculations. In this study, we propose an improvement in the algorithm of the TP method that results in a much better agreement over FYI with the LLE method, i.e. with differences reduced to less than 2 cm on average. Therefore, we would recommend using the TP method with our improved algorithm over the LLE method to calculate local sea surface references as it is based on a physical relationship and seems adequate to give reasonable results over both MY and FY areas.

The freeboard corrections that have been applied in the last release of the JPL product to account for snow depth in leads and for leads width with respect to the size of the ICESat altimeter footprint (Kwok and Cunningham, 2008; Kwok et al., 2009) are significantly impacting the freeboard values estimated using the TP method, accounting for an increase of about 7cm in average.

We show that the different along-track averaging scales and approaches to calculate sea surface references, from one side, and the freeboard adjustments as applied in the TP method used to produce the JPL dataset, from the other side, are roughly compensating each other with respect to freeboard estimation. Indeed, we obtain similar freeboard estimates while using the TP and LLE methods with the set of parameters used by Kwok et al. (2009) and Yi and Zwally 2009, respectively. We therefore suspect that the differences found in the JPL and GSFC sea ice thickness products are not intrinsically due to the difference in the freeboard retrieval methods, but may be attributed to the use of differences in the freeboard-to-thickness conversion.

Acknowledgments. This work was funded and supported by the Nansen Environmental and Remote Sensing Center and by the ESA Climate Change Initiative, Sea Ice project (SICCI).

References

Farrell S. L., Laxon S. W., McAdoo D. C., Yi D and Zwally H. J.: Five years of Arctic sea ice freeboard measurements from the Ice, Cloud and land Elevation Satellite. J. Geophys. Res.,114(C4):C04008. doi:10.1029/2008JC005074, 2009.

Kern S. and Spreen G.: Uncertainties in Antarctic sea-ice thickness retrieval from ICESat, Ann. Glaciol., 6(69), 107-119, doi:10.3189/2015AoG69A736, 2015.

Kurtz N. T. and Markus T.: Satellite observations of Antarctic sea ice thickness and volume, J. Geophys. Res., 117, C08025, doi:10.1029/2012JC008141, 2012.

Kurtz N. T., Markus T., Cavalieri D. J., Sparling L. C., Krabill W. B., Gasiewski A. J. and Sonntag J. G.:. Estimation of sea ice thickness distributions through the combination of snow depth and satellite laser altimetry data. J. Geophys. Res. Ocean, 114, C10007, doi:10.1029/2009JC005292, 2009.

Kurtz N. T., Markus T., Farrell S. L., Worthen D. L. and Boisvert L. N.: Observations of recent Arctic sea ice volume loss and its impact on ocean-atmosphere energy exchange and ice production, J. Geophys. Res., 116, C04015, doi:10.1029/2010JC006235, 2011.

Kwok R.: Annual cycles of multiyear sea ice coverage of the Arctic Ocean: 1999–2003, J. Geophys. Res., 109, C11004, doi:10.1029/2003JC002238, 2004.

Kwok R. and Cunningham G. F.: ICESat over Arctic sea ice: estimation of snow depth and ice thickness. J. Geophys. Res., 113(C8), C08010, doi: 10.1029/2008JC004753, 2008.

Kwok R, Zwally H. J. and Yi D.: ICESat observations of Arctic sea ice: a first look. Geophys. Res. Lett., 31(16), L16401 (doi:10.1029/2004GL020309), 2004.

Kwok R., Cunningham G. F., Zwally H. J. and Yi D.: ICESat over Arctic sea ice: Interpretation of altimetric and reflectivity profiles, J. Geophys. Res., 111, C06006, doi:10.1029/2005JC003175, 2006.

Kwok R., Cunningham G. F., Zwally H. J. and Yi D.: Ice, Cloud, and land Elevation Satellite (ICESat) over Arctic sea ice: Retrieval of freeboard, J. Geophys. Res., 112, C12013, 2007.

Kwok R., Cunningham G. F., Wensnahan M., Rigor I., Zwally H. J. and Yi D.: Thinning and volume loss of the Arctic Ocean sea ice cover: 2003–2008, J. Geophys. Res., 114, C07005, doi:10.1029/2009JC005312, 2009.

Laxon S., Peacock N. and Smith D.: High interannual variability of sea ice thickness in the Arctic region, Nature, 425(6961), 947-950, 2003.

Laxon S. W., Giles K. A., Ridout A. L., Wingham D. J., Willatt R., Cullen R., Kwok R., Schweiger A., Zhang J., Haas C., Hendricks S., Krishfield R., Kurtz N., Farrell S. and Davidson M.: CryoSat-2 estimates of Arctic sea ice thickness and volume, Geophys. Res. Lett., 40, 732-737, doi:10.1002/grl.50193, 2013.

Lindsay R. and Schweiger A.: Arctic sea ice thickness loss determined using subsurface, aircraft, and satellite observations, The Cryosphere, 9(1), 269-283, doi:10.5194/tc-9-269-2015, 2015.

Markus T., Massom R., Worby A., Lytle V., Kurtz N. and Maksym T.: Freeboard, snow depth and sea-ice roughness in East Antarctica from in situ and multiple satellite data, Ann. Glaciol., 52(57), 242-248, 2011.

Pavlis N. K. , Holmes S. A., Kenyon S. C. and Factor J. K.: The development and evaluation of the Earth Gravitational Model 2008 (EGM2008), J. Geophys. Res., 117, B04406, doi:10.1029/2011JB008916, 2012.

Ricker R., Hendricks S., Helm V., Skourup H. and Davidson M.: Sensitivity of Cryosat-2 Arctic sea-ice freeboard and thickness on radar-waveform interpretation, The Cryosphere, 8, 1607–1622, doi:10.5194/tc-8-1607-2014, 2014.

Stocker T. F., Dahe Q. nad Plattner G. K.: Climate Change 2013: The Physical Science Basis, Intergovernmental Panel on Climate Change 2013, 2013.

Tilling, R. L., Ridout, A., Shepherd, A. and Wingham, D. J.: Increased Arctic sea ice volume after anomalously low melting in 2013, Nature Geoscience, 8, 643-646, 2015.

Vaughan, D., Comiso, J., Allison, I., Carrasco, J., Kaser, G., Kwok, R., Mote, P., Murray, T., Paul, F., Ren, J., Rignot, E., Solomina, O., Steffen, K., and Zhang, T.: Observations: Cryosphere, book section 4, 317–382, Cambridge University Press, Cambridge, United Kingdom and New York, NY, USA, doi:10.1017/CBO9781107415324.012, www.climatechange2013.org, 2013.

Yi D. and Zwally H. J.: Arctic Sea Ice Freeboard and Thickness, National Snow and Ice Data Center, Boulder, Colorado, USA, 2009, 2014-04-15.

Yi D., Zwally H. J. and Robbins J. W.: ICESat observations of seasonal and interannual variations of sea-ice freeboard and estimated thickness in the Weddell Sea, Antarctica (2003 – 2009), 52, 43-51, 2011.

Zwally H. J., Yi D., Kwok R. and Zhao Y.: ICESat measurements of sea ice freeboard and estimates of sea ice thickness in the Weddell Sea, J. Geophys. Res., 113, C02S15, doi:10.1029/2007JC004284, 2008.

Zygmuntowska M., Rampal P., Ivanova N. and Smedsrud L. H.: Uncertainties in Arctic sea ice thickness and volume: new estimates and implications for trends, The Cryosphere, 8, 705-720, doi:10.5194/tc-8-705-2014, 2014.

Table 1. Mean/std of the differences between freeboards estimated using different averaging scales and geoids (cm). The compared methods are indicated by the used geoid (ArcGP or EGM08), geoid adjustment is indicated by dif, scale of along-track averaging is indicated by 50 (i.e. applying of 50-km and 100-km windows for estimating of $\bar{h}$ and h_{sl}) and 25 ((i.e. applying of 25-km windows for estimating of $\bar{h}$ and h_{sl}).

Methods compared	ON03	FM04	ON04	FM05	ON05	FM06	ON06	MA07	ON07	FM08
ArcGP/dif/50 – GSFC	0.3/6.5	0.4/5.6	0.6/6.7	1.2/7.3	-1.5/6.6	0.1/5.7	-1.7/6.5	-0.3/5.9	-2.0/7.2	-0.4/5.7
ArcGP/dif/50 (gain 80) – GSFC	4.6/12.4	1.3/5.5	4.6/9.2	3.1/8.6	1.9/6.3	1.7/5.5	1.4/5.5	1.5/5.5	2.8/6.0	1.2/5.2
EGM08/50 – EGM08/25	5.2/8.8	3.6/7.3	5.7/8.4	6.4/9.1	3.7/7.8	3.8/7.5	3.3/6.6	3.8/7.7	4.1/8.4	3.8/8.6
EGM08/dif/50 – EGM08 / 50	0.1/5.2	0.7/4.2	0.0/5.2	0.2/7.0	0.3/4.8	0.7/3.9	0.3/4.6	0.5/4.4	0.0/4.7	0.5/3.8
EGM08/50 – ArcGP /50	0.0/3.7	0.2/2.7	0.0/3.2	0.2/2.7	0.1/3.0	0.2/2.8	0.1/3.1	0.2/2.7	0.0/5.9	0.2/2.7

Table 2. Adjustments of sea ice freeboard retrieved by the TP method to account for snow depth in refrozen leads and for leads size with respect to the size of the ICESat footprint. The adjustments are estimated following the methods described in Kwok and Cunningham (2008) and Kwok et al., (2009).

Correction	ON03	FM04	ON04	FM05	ON05	FM06	ON06	MA07	ON07	FM08
Snow depth	2.5/1.0	3.0/1.0	2.8/1.0	3.0/1.0	2.7/1.1	2.7/1.1	2.7/1.2	2.9/1.2	2.3/1.3	2.6/1.1
Leads width	4.5/2.3	3.1/1.7	6.1/3.1	6.9/3.3	4.1/2.4	4.1/2.2	3.3/1.9	3.6/1.9	3.2/1.8	2.6/1.6

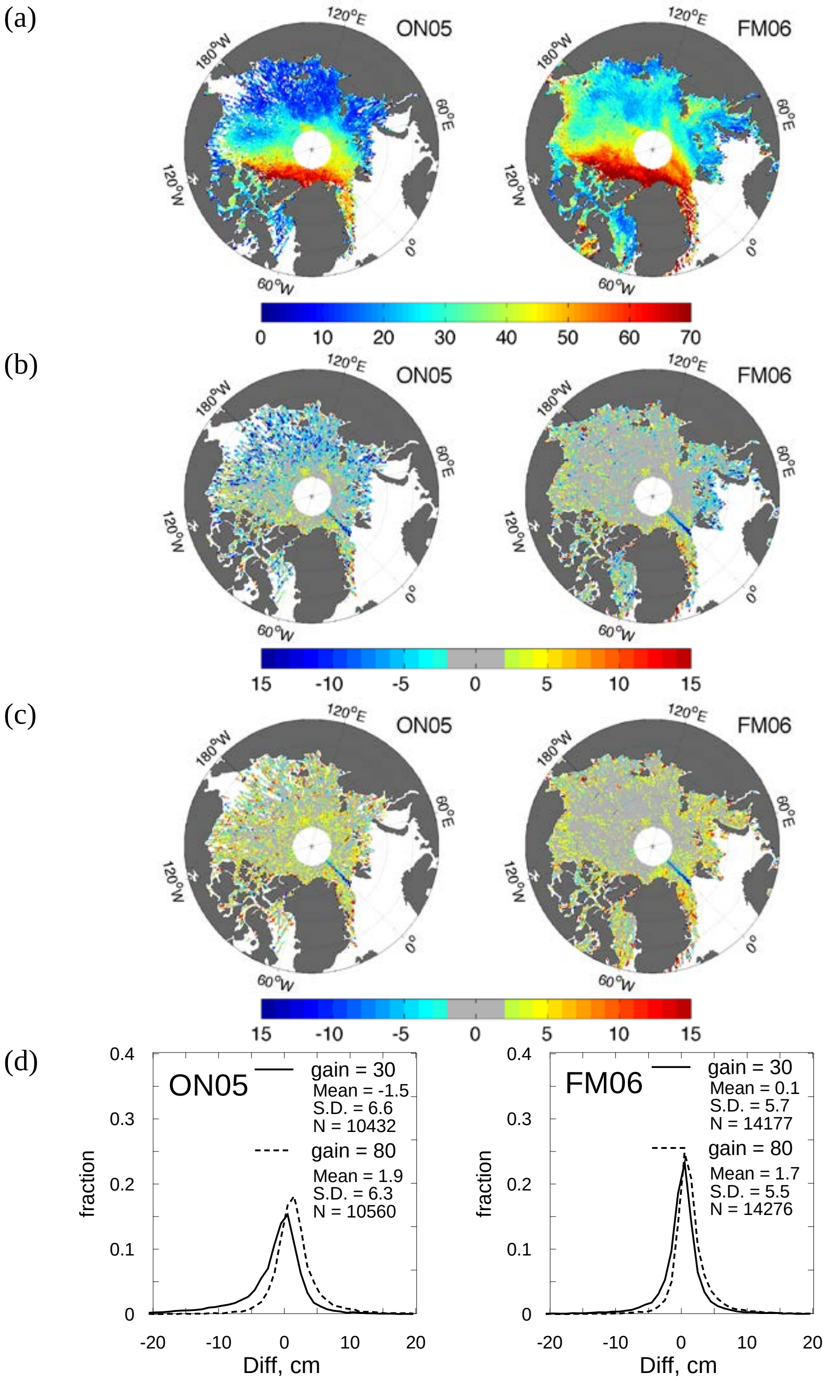
(a)
ON05
FM06
120°E
180°W
60°E
120°W
0°
60°W
0 10 20 30 40 50 60 70
(b)
ON05
FM06
15 -10 -5 0 5 10 15
(c)
ON05
FM06
15 -10 -5 0 5 10 15
(d)
ON05
gain = 30
Mean = -1.5
S.D. = 6.6
N = 10432
gain = 80
Mean = 1.9
S.D. = 6.3
N = 10560
FM06
gain = 30
Mean = 0.1
S.D. = 5.7
N = 14177
gain = 80
Mean = 1.7
S.D. = 5.5
N = 14276
fraction
0 0.1 0.2 0.3 0.4
-20 -10 0 10 20
Diff, cm

Figure 1. (a) Freeboard retrieved by the LLE method using along-track averaging scales as applied by Yi and Zwally (2009) to derive the GSFC product and (b-d) its differences from the GSFC freeboards (freeboads from this study minus GSFC freeboards) for ON05 and FM06 periods gridded into 25-km bins (cm). The freeboards estimated in this study are obtained using ICESat data with receiver gain of smaller than 30 (b) and 80 (c). (d) Distribution of the differences between freeboards.

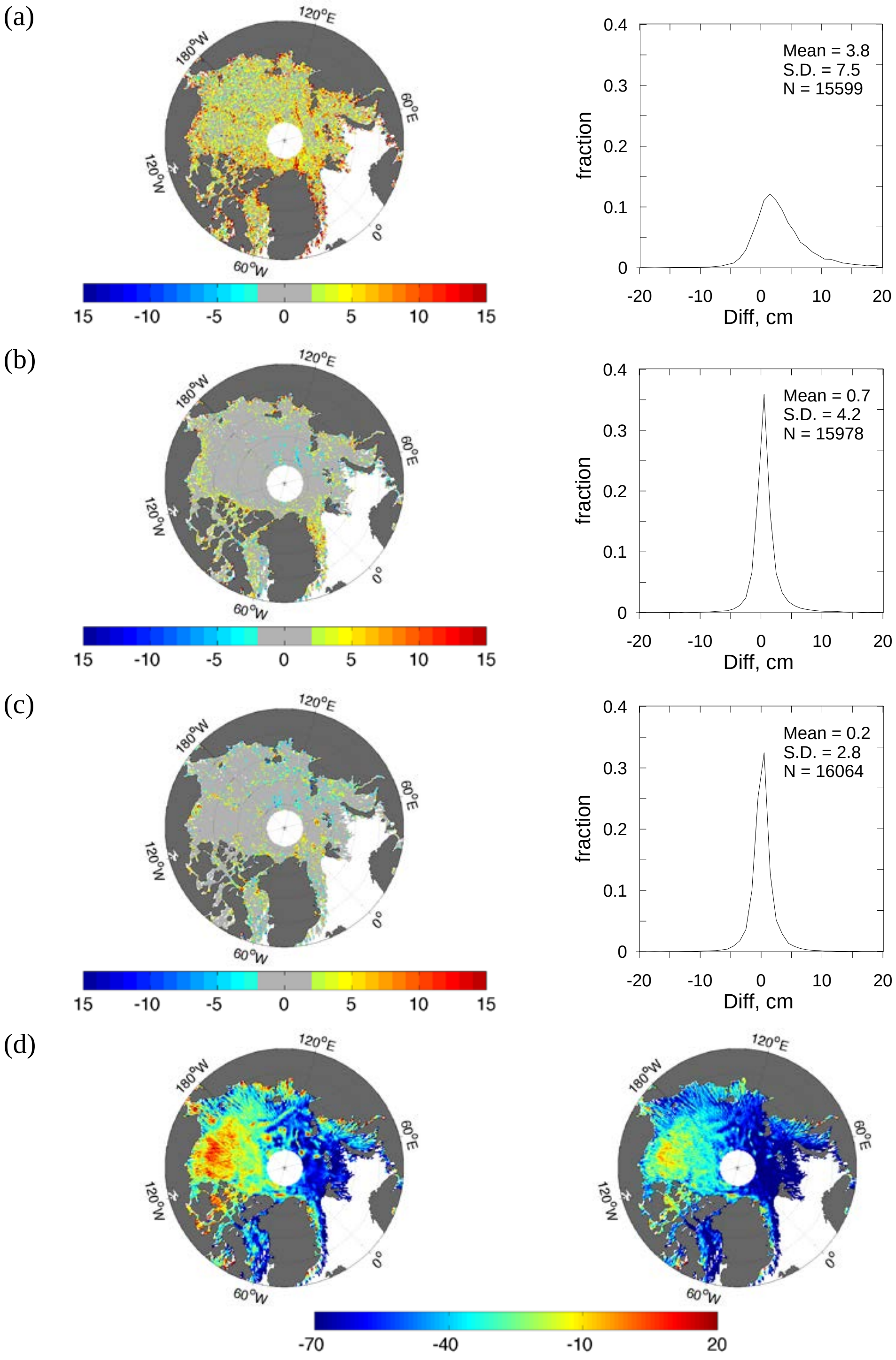
(a)
120°E
180°W
60°E
120°W
0°
60°W
15
-10
-5
0
5
10
15
0.4
0.3
0.2
0.1
0
fraction
Mean = 3.8
S.D. = 7.5
N = 15599
-20
-10
0
10
20
Diff, cm
(b)
Mean = 0.7
S.D. = 4.2
N = 15978
(c)
Mean = 0.2
S.D. = 2.8
N = 16064
(d)
-70
-40
-10
20

Figure 2. Effect of using different geoids and scales for along-track averaging on freeboard estimates (cm) when applying the LLE method for FM06 period (25-km grids). Differences between freeboard estimates show the effects of (a) applying longer and shorter along-track averaging scales (longer minus shorter) when using EGM08 geoid as well as (b) adjustment of ArcGP geoid for $\bar{h} - h_{sl}$ values (adjusted minus unadjusted) and (c) using different geoids (EGM08 minus ArcGP) in case of applying longer along-track averaging scales.

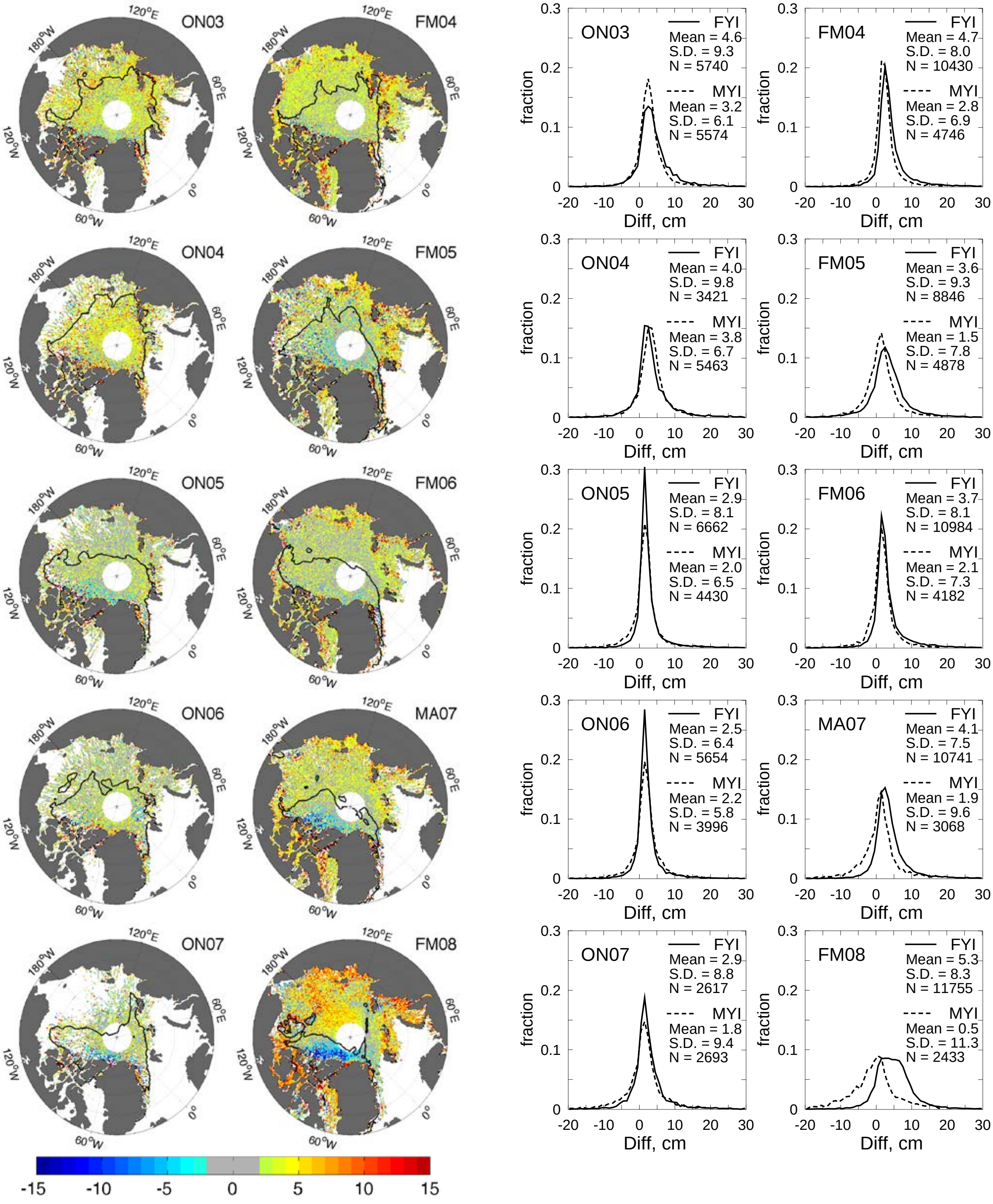
ON03
FM04
ON04
FM05
ON05
FM06
ON06
MA07
ON07
FM08
120°E
180°W
60°E
120°W
0°
60°W
-15
-10
-5
0
5
10
15
ON03: FYI Mean = 4.6, S.D. = 9.3, N = 5740; MYI Mean = 3.2, S.D. = 6.1, N = 5574
FM04: FYI Mean = 4.7, S.D. = 8.0, N = 10430; MYI Mean = 2.8, S.D. = 6.9, N = 4746
ON04: FYI Mean = 4.0, S.D. = 9.8, N = 3421; MYI Mean = 3.8, S.D. = 6.7, N = 5463
FM05: FYI Mean = 3.6, S.D. = 9.3, N = 8846; MYI Mean = 1.5, S.D. = 7.8, N = 4878
ON05: FYI Mean = 2.9, S.D. = 8.1, N = 6662; MYI Mean = 2.0, S.D. = 6.5, N = 4430
FM06: FYI Mean = 3.7, S.D. = 8.1, N = 10984; MYI Mean = 2.1, S.D. = 7.3, N = 4182
ON06: FYI Mean = 2.5, S.D. = 6.4, N = 5654; MYI Mean = 2.2, S.D. = 5.8, N = 3996
MA07: FYI Mean = 4.1, S.D. = 7.5, N = 10741; MYI Mean = 1.9, S.D. = 9.6, N = 3068
ON07: FYI Mean = 2.9, S.D. = 8.8, N = 2617; MYI Mean = 1.8, S.D. = 9.4, N = 2693
FM08: FYI Mean = 5.3, S.D. = 8.3, N = 11755; MYI Mean = 0.5, S.D. = 11.3, N = 2433
fraction
0
0.1
0.2
0.3
Diff, cm
-20
-10
0
10
20
30

Figure 3. Maps (left) and distributions (right) of the differences between sea ice freeboard (25-km grids) estimated using LLE and TP methods (LLE minus TP) for ten ICESat periods (cm). Thick black line on the maps delineates the average 50% isopleth of multi-year ice fraction.

5

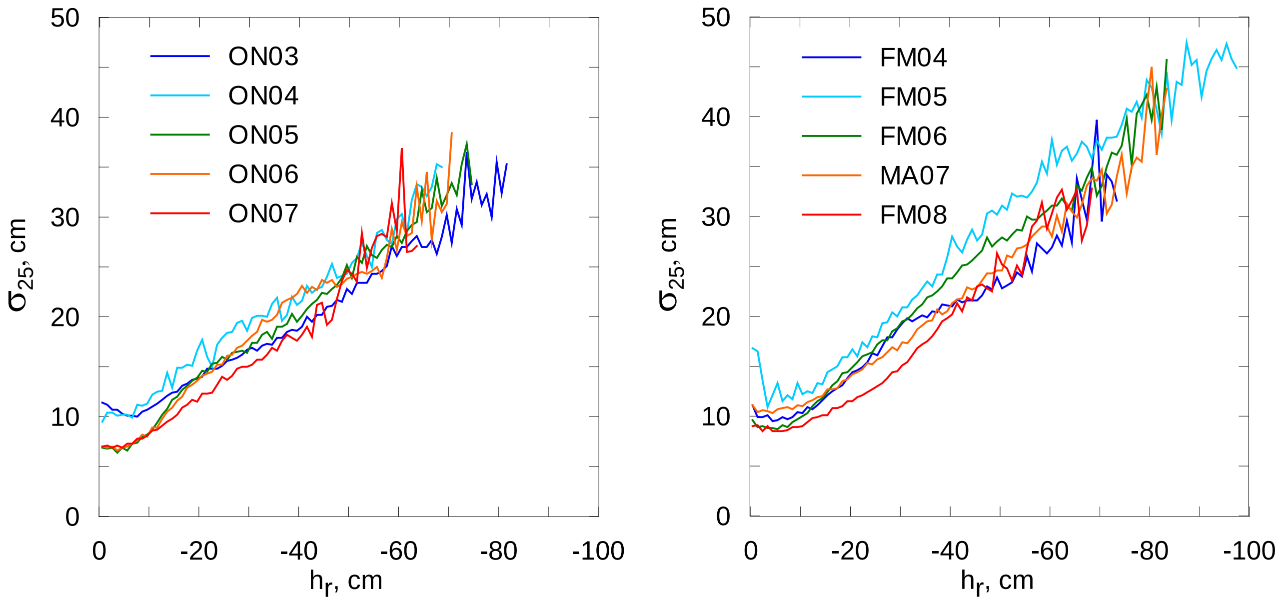

Figure 4. The relationships between $\mathrm{h_r}$ and σ_{25}, for samples where dips in reflectivity is measured for fall (a) and winter (b) ICESat periods, following the method described in Kwok et al. (2007). The $\mathrm{h_r}$ axis is discretized in bins of 1-cm. Note that following Zwally et al. (2008) and Yi and Zwally (2009) we define $\mathrm{h_r}$ as $h_r = h - \bar{h}$ and form the relationship for negative $\mathrm{h_r}$ values, while in Kwok et al. (2007) $h_r = \bar{h} - h$ and positive $\mathrm{h_r}$ values are considered.

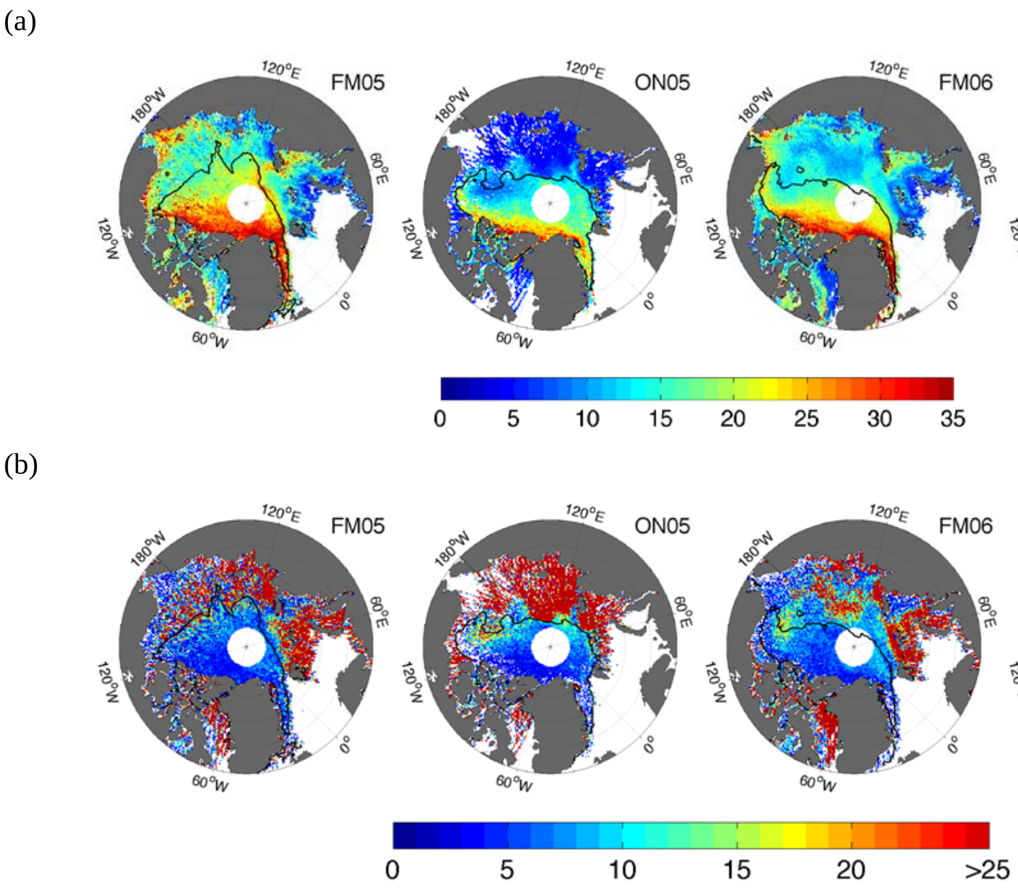

Figure 5. Standard deviation of detrended elevations h_r (cm) (a) and number of tiepoints within 25-km non-overlapping segments detected by the TP method (b) for FM05, ON05, FM06 and FM08 periods.

The Cryosphere Discuss., doi:10.5194/tc-2016-50, 2016
Manuscript under review for journal The Cryosphere
Published: 6 April 2016

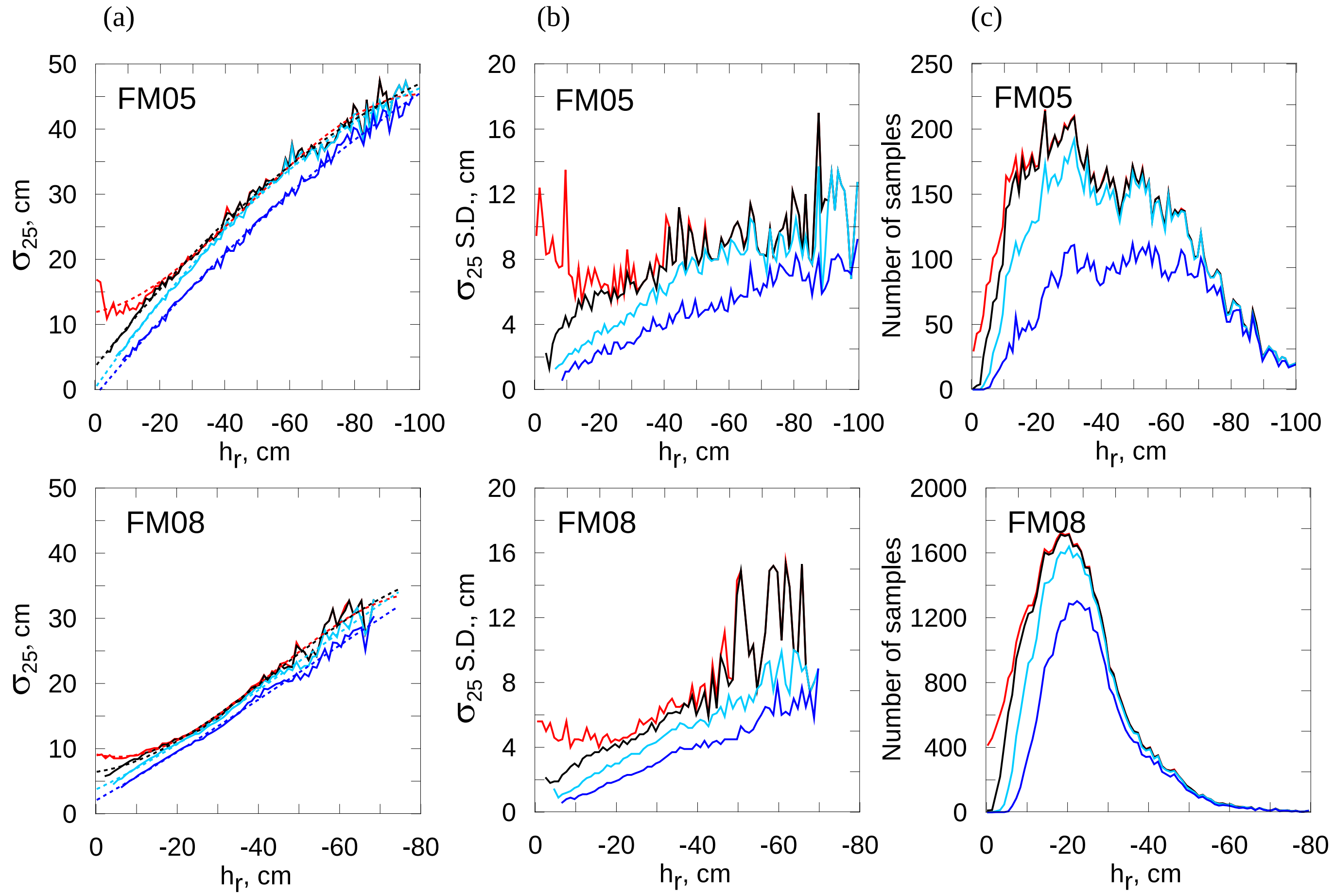

Figure 6. The relationship between h_r and σ_{25} (a), distributions of its standard deviations (b), and number of samples in each h_r bin (c) for FM05 and FM08 ICESat periods. Red lines are constructed from the selection of samples for which dips in reflectivity are measured, as described in (Kwok et al., 2007). Black, cyan and blue lines are constructed from the new selection of samples we propose in this study, based on requesting the presence of dips in both reflectivity and elevation measurements (See text for details).

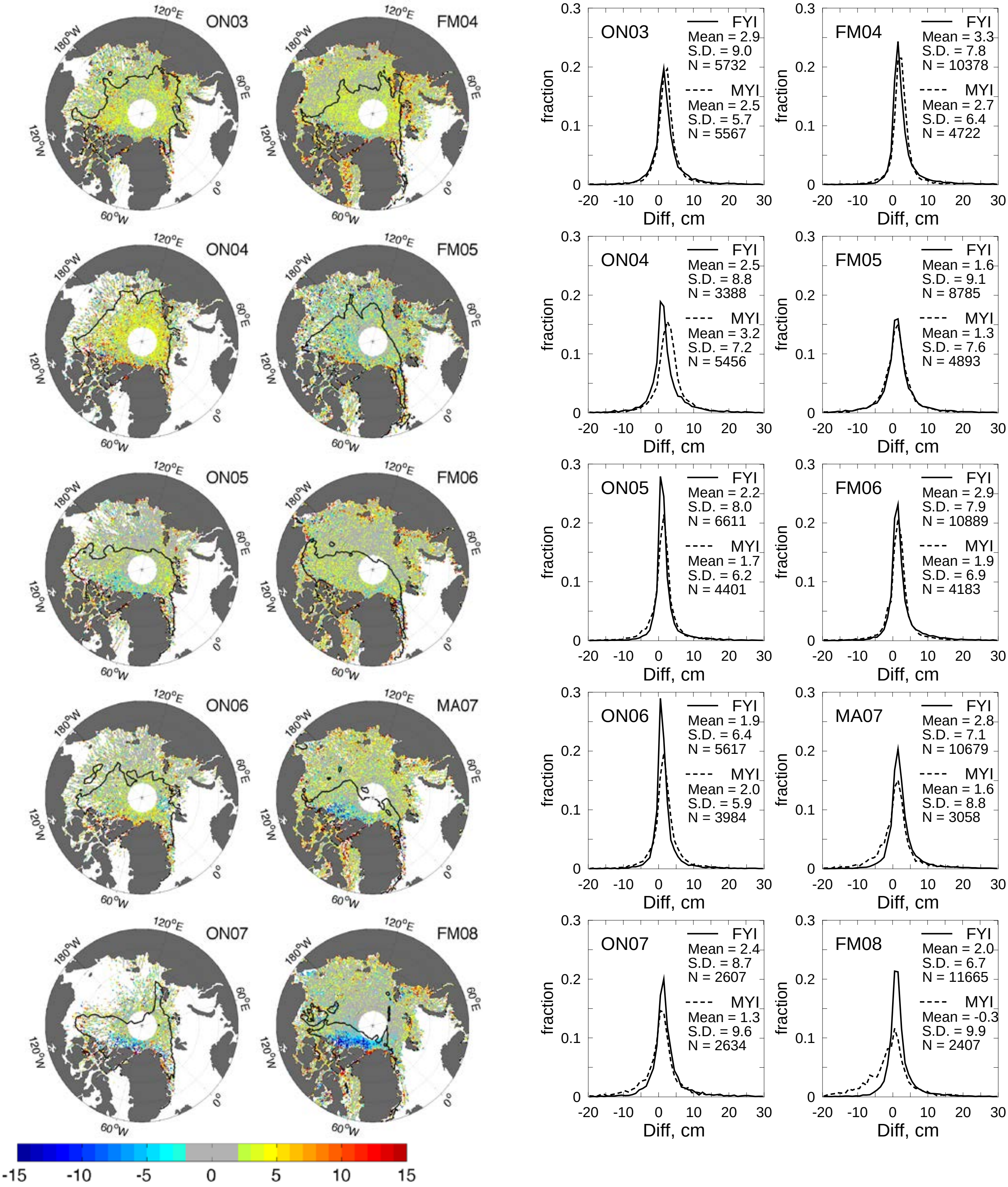
ON03
FM04
ON04
FM05
ON05
FM06
ON06
MA07
ON07
FM08
120°E
180°W
60°E
120°W
0°
60°W
-15
-10
-5
0
5
10
15
fraction
Diff, cm
0.3
0.2
0.1
0
-20
-10
0
10
20
30
ON03: FYI Mean = 2.9 S.D. = 9.0 N = 5732; MYI Mean = 2.5 S.D. = 5.7 N = 5567
FM04: FYI Mean = 3.3 S.D. = 7.8 N = 10378; MYI Mean = 2.7 S.D. = 6.4 N = 4722
ON04: FYI Mean = 2.5 S.D. = 8.8 N = 3388; MYI Mean = 3.2 S.D. = 7.2 N = 5456
FM05: FYI Mean = 1.6 S.D. = 9.1 N = 8785; MYI Mean = 1.3 S.D. = 7.6 N = 4893
ON05: FYI Mean = 2.2 S.D. = 8.0 N = 6611; MYI Mean = 1.7 S.D. = 6.2 N = 4401
FM06: FYI Mean = 2.9 S.D. = 7.9 N = 10889; MYI Mean = 1.9 S.D. = 6.9 N = 4183
ON06: FYI Mean = 1.9 S.D. = 6.4 N = 5617; MYI Mean = 2.0 S.D. = 5.9 N = 3984
MA07: FYI Mean = 2.8 S.D. = 7.1 N = 10679; MYI Mean = 1.6 S.D. = 8.8 N = 3058
ON07: FYI Mean = 2.4 S.D. = 8.7 N = 2607; MYI Mean = 1.3 S.D. = 9.6 N = 2634
FM08: FYI Mean = 2.0 S.D. = 6.7 N = 11665; MYI Mean = -0.3 S.D. = 9.9 N = 2407

Figure 7. Maps (left) and distributions (right) of the differences between sea ice freeboard (25-km grids) estimated using LLE and TP methods (LLE minus TP) for ten ICESat periods (cm). The TP method used here includes the improvements in the freeboard retrieval algorithm proposed in this study. Thick line on the maps delineates the 50% isopleth of multi-year ice fraction.

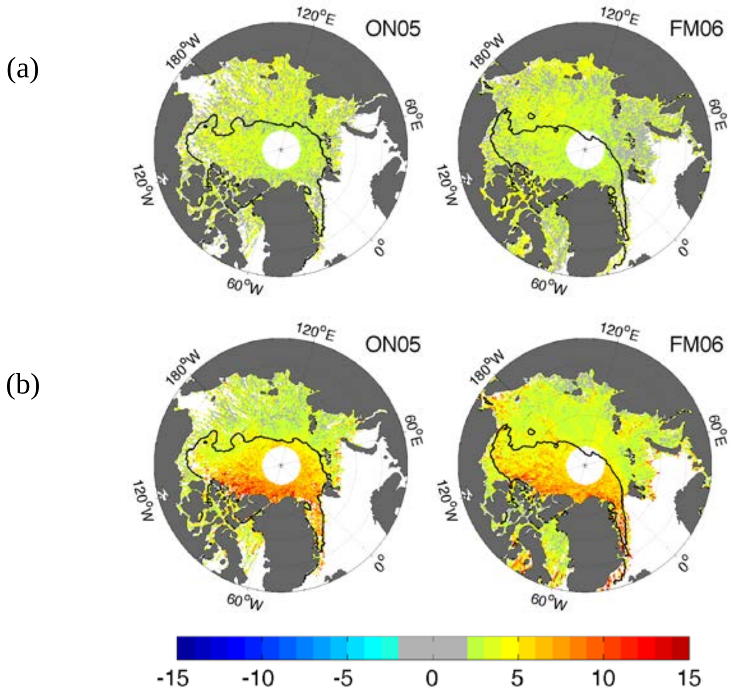

Figure 8. Adjustments of freeboard retrieved using the TP method accounting for (a) snow depth on top of new ice in leads and (b) leads width with respect to ICESat footprint area for the periods ON05 and FM06. These adjustments are estimated following the methods described in Kwok and Cunningham (2008) and Kwok et al. (2009).

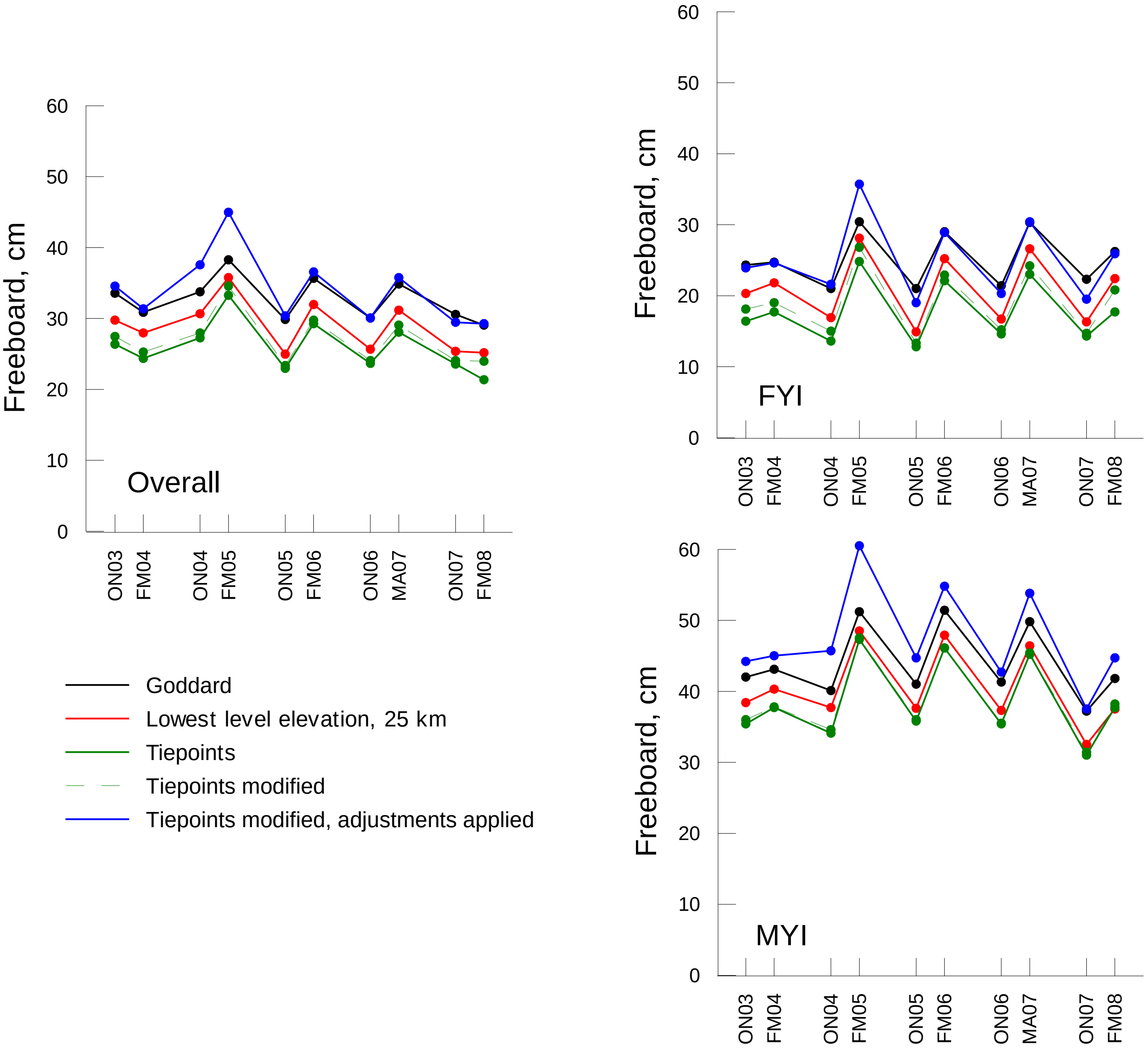

Figure 9. Freeboard time series calculated over the whole arctic basin, FYI and MYI areas as provided in the GSFC product (black) and retrieved in this study by the LLE method when using shorter along-track averaging scales (red), the TP method (green), the TP method, which includes the improvements in the freeboard retrieval algorithm proposed in this study without (green dashed) or with (blue) adjustments for snow depth and leads width applied.